Research Article | Vol. 11, No. 9 / 1 September 2020 / Biomedical Optics Express 4862
Biomedical Optics EXPRESS

HER2 biosensing through SPR-envelope tracking in plasmonic optical fiber gratings

Maxime Lobry,[1,5,*] Médéric Loyez,[2] Karima Chah,[1] Eman M. Hassan,[3,4] Erik Goormaghtigh,[5] Maria C. DeRosa,[3] Ruddy Wattiez,[2] and Christophe Caucheteur[1]

[1]*Electromagnetism and Telecommunication Department, University of Mons, 31 Bld Dolez, 7000 Mons, Belgium*
[2]*Proteomics and Microbiology Department, University of Mons, 6 Av. du Champ de Mars, 7000 Mons, Belgium*
[3]*Institute of Biochemistry, Carleton University, 1125 Colonel By Drive, Ottawa, Ontario, K1S 5B6, Canada*
[4]*Metrology Research Centre, National Research Council Canada, Ottawa, Ontario, K1A0R6, Canada*
[5]*Laboratory for the Structure and Function of Biological Membranes, Center for Structural Biology and Bioinformatics, Université Libre de Bruxelles, Bld du Triomphe 2,1050 Brussels, Belgium*
[*]*maxime.lobry@umons.ac.be*

Abstract: In the biomedical detection context, plasmonic tilted fiber Bragg gratings (TFBGs) have been demonstrated to be a very accurate and sensitive sensing tool, especially well-adapted for biochemical detection. In this work, we have developed an aptasensor following a triple strategy to improve the overall sensing performances and robustness. Single polarization fiber (SPF) is used as biosensor substrate while the demodulation is based on tracking a peculiar feature of the lower envelope of the cladding mode resonances spectrum. This method is highly sensitive and yields wavelength shifts several tens of times higher than the ones reported so far based on the tracking of individual modes of the spectrum. An amplification of the response is further performed through a sandwich assay by the use of specific antibodies. These improvements have been achieved on a biosensor developed for the detection of the HER2 (*Human Epidermal Growth Factor Receptor-2*) protein, a relevant breast cancer biomarker. These advanced developments can be very interesting for point-of-care biomedical measurements in a convenient practical way.

1. Introduction

In the scope of detection, optical fiber sensors find their place in a lot of applications involving real-time and continuous monitoring [1–3]. The area of implantation is very wide with plenty of opportunities, in particular for the development of strain, temperature, pressure, chemical and bio-chemical sensors [4–9]. Many interesting ways exist to achieve the development of an optical fiber sensor for which the most frequently encountered designs include unclad fibers, U-bent fibers [10], etched fibers [11], tapered fibers [12] and fiber gratings [4–6,13–15]. In these aforementioned configurations, tilted fiber Bragg gratings (TFBGs) represent a particularly convenient and relevant solution for biochemical and/or medical sensing once coupled to surface plasmon resonance (SPR) and bioreceptors immobilization (antibodies, aptamers, enzymes, etc) [16–20]. This refractive index modulation inscribed within the fiber couples light out the core and makes this waveguide sensitive to the outer medium. An enhancement of surface sensitivity can be obtained through the excitation of an SPR, an excited and collective oscillation of electrons, when a thin metal overlay is deposited over the TFBG and when appropriate light polarization is injected. An SPR-TFBG sensor represents then a highly tunable and versatile platform allowing the development of highly accurate and sensitive biosensing tools. In fact, such a device already proved its high potential, efficiency, and performances in biosensing, since miscellaneous biorecognition strategies can be considered depending on the target analyte

#401200 https://doi.org/10.1364/BOE.401200
Journal © 2020 Received 26 Jun 2020; revised 22 Jul 2020; accepted 22 Jul 2020; published 4 Aug 2020

Biomedical Optics EXPRESS

(proteins, lipids, enzymes, DNA, cells, etc). It also benefits from the numerous advantages provided when working with optical fibers. The development of a fully biocompatible, flexible, cost-effective and small-scaled (diameter of 125 µm only) optrode for minimally invasive and real-time *in-situ* detection in very small volumes (~100 µl) is entirely possible [12,19].

Breast cancer represents the most common cancer in women and occupies the second place in terms of number of cancer deaths worldwide just after lung and bronchus cancers [21]. For these pathologies, this number is directly imputed to late diagnosis and widespread of metastases. Nowadays, breast cancer tumor examinations rely on mammography, magnetic resonance imaging (MRI) and ultrasound or positron emission tomography (PET-scans). In the case of breast cancer diagnosis, the determination of the HER2 (*Human Epidermal Growth Factor Receptor-2*) status plays a key role in medical decisions for the choice of medicines and treatments [22]. The receptor tyrosine-kinase HER2 (also referred to as HER2/neu or Erb-B2) is a transmembrane protein which helps to manage the growth, the mitosis, and the repair of healthy breast cancer cells. However, the overexpression of this protein onto breast cell wall due to an abnormal HER2 gene amplification leads to an uncontrolled cell growth and mitosis, i.e. to a cancer. These phenomena result from different cell signalization pathways in the form of a downstream of phosphorylations/dephosphorylations through the epithelial cell when the HER2 receptor is activated. The phosphoinositide 3-kinase/Protein Kinase B (PI3K/AKT) [23] and the RAF/MEK/MAPK pathways are the most solicited [24]. The detection of HER2 in particular is very relevant because breast cancers involving HER2 protein overexpression, also known as HER2-positive (HER2+) breast cancer, tend to be more aggressive with a more rapid progression and a higher propensity to come back in comparison with HER2-negative (HER2-) ones [25]. HER2+ patients are generally treated with tyrosine kinase inhibitors (TKIs) such as trastuzumab [26]. In routine, the amount of HER2 proteins is determined through IHC test (ImmunoHistoChemistry) or with a FISH test (Fluorescence In Situ Hybridization) when the first method conducts to borderline results [22,26]. The major drawbacks of these techniques are their invasiveness involving numerous biopsies to avoid misdiagnosis and their relatively long processing time. In contrast, an optical fiber-based biosensor has the capability to yield minimally-invasive measurements and real-time operation.

To date, most of experiments involving plasmonic TFBGs have been based on standard telecommunication-grade single-mode optical fibers (SMFs), offering easy light injection with a cost-effective equipment. SPR can be excited through the use of P-polarized light, which implies finely adjusting the input state of polarization and preserving it by avoiding any unwanted polarization instabilities, as done in our previous works [13,19,20,27]. In the context of early pathology diagnosis, there is still room for practical performance improvement. In this work, we have contributed to this development, following a triple approach: use of another fiber type (1), set-up of a user-friendly demodulation technique (2) and sandwich bioassay (3). We have selected a single polarization fiber (SPF) that provides several interesting practical features. Indeed, the chosen SPF is a highly birefringent bow-tie fiber especially designed to strongly attenuate one of the two orthogonal states of polarization. At the expenses of a higher price per unit of length compared to the standard SMF, the P-polarization state propagation is highly fostered with a very positive impact on the SPR signal. A clean SPR signature is obtained with a high tolerance to polarization instabilities caused by optical fiber cable movements, which improves the robustness of experimental measurements and the quality of point-of-care biodetection. HER2 cancer biomarker detection is performed by a demodulation technique based on the tracking of the SPR signature envelope fit. This method can be easily automated and brings a very high sensitivity to surface events. For bioassays, thiolated aptamers were first directly immobilized onto the sensor surface for the label-free detection of HER2. Anti-HER2 antibodies were then added as amplifiers to significatively improve the sensitivity. Here, and contrary to our previous reports, we did not work towards the quantification of the actual limit of detection. As aforementioned, our motivation was to strengthen the practicability of a highly sensitive biosensing platform.

Biomedical Optics EXPRESS

2. Development of SPR TFBG-based SPF aptasensor

2.1. SPR TFBG sensor

TFBG is a periodic modulation of the refractive index (RI) featuring a slight angle (1-10°) with respect to the perpendicular to the fiber axis [28–30]. This structure is generally inscribed within the fiber core under side laser radiation with the use of a tilted phase mask [31–33]. The TFBG acts as a set of tilted mirrors that breaks the fiber core symmetry and outcouples a part of the core guided light in the fiber cladding. Only for some defined wavelengths, the coupling phase-matching conditions are fulfilled [29,30,34] and give rise to several narrow resonances in the transmission TFBG spectrum. These cladding modes are directly in contact with the outer medium-cladding interface and are therefore sensitive to (SRI) changes [4,12,28,35]. The Bragg core mode, which appears at the right extremity of the TFBG transmission spectrum, is only sensitive to temperature and/or strain variations. This mode can be exploited to compensate for these disturbing effects while measuring SRI. A TFBG can therefore be considered as a self-referenced system. The sensitivity to SRI can be easily and highly enhanced by covering the grating area with a thin and finely tuned metal sheath (~30–50 nm). A gold layer is preferred for stainless and biocompatibility reasons and its dielectric constant value well-suited for SPR excitation [12,36,37]. An SPR is an oscillation of electrons occurring at a metal-dielectric interface and generating a surface evanescent wave which locally amplifies the electric field close to the fiber surface. To achieve this, the incident light at the metal-dielectric interface must be radially-polarized (P-polarization) with an identical tangential component to that of the plasmon wave [12,37]. This phenomenon improves the sensor sensitivity to a depth of ~λ/3 to λ/2, which explains the extensive use of SPR excitation for biosensing purposes [14,16,38–40]. In practice, a linear polarizer is used upstream of the TFBG in single mode fiber to select the right polarization for SPR excitation. In standard SMF28, the light polarization is not maintained, implying to secure the connecting fibers once the proper state of polarization is adjusted.

In this study, TFBGs are produced in single polarization fiber (SPF). This type of fiber allows for the propagation of a single mode with the specific and required polarization to excite the SPR. This polarization maintaining fiber is based on extremely birefringent bow-tie design from Fibercore (Zing HB1550Z) with core and cladding diameters of 11 and 125 µm, respectively. The fiber can either polarize unpolarized light or improve the polarization of an existing light source in a range of 100 nm around 1550 nm. Gratings are inscribed with a 193 nm ArF excimer laser and the phase mask technique. The latter is implemented thanks to a NORIA system (NorthLab Photonics, Sweden). The fiber is firstly hydrogenated (200 bar, 60 °C, 30h) in order to amplify the photosensitivity of the Ge-doped fiber core. The grating stability is significantly improved by performing a thermal annealing at 100 °C for 24 hours. The fiber at the grating location is then covered with a thin gold metal layer of ~35 nm by the means of a sputtering process (Leica EM SCD 500), allowing SPR excitation which increases the sensitivity of the biodetection. This gold thickness results from one of our previous study [37] which was found to be a right trade-off to access to a very sensitive and clean SPR signal. The gold layer is locally heated (200 °C, 2h) to ensure its adhesion on the silica fiber surface.

2.2. Aptamer immobilization and setup

The plasmonic sensor is biofunctionalized by immobilizing thiolated anti-HER2 ssDNA aptamers directly onto the gold surface through covalent bounds in order to specifically detect HER2 breast cancer biomarkers (Fig. 1). These aptamers were selected by the Systematic Evolution of Ligands by EXponential enrichment (SELEX) method with sequence Ref. He_A2_3 [41]. The thiolated anti-HER2 aptamers (5'-TCT AAA AGG ATT CTT CCC AAG GGG ATC CAA TTC AAA CAG C-S-S-3') were then synthetized by using a MerMade 6 automated DNA synthesizer (BioAutomation USA) [41–43]. DNA bases and thiol modifiers come from Glen Research (Sterling, VA, USA).

Biomedical Optics EXPRESS

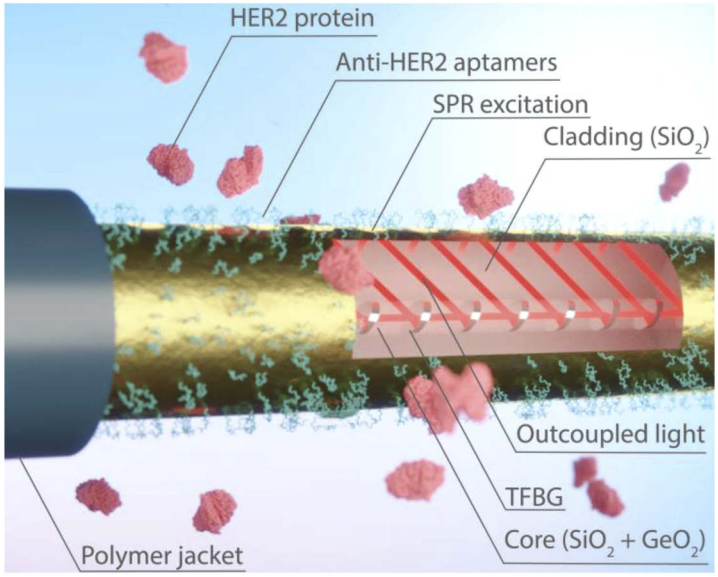

Fig. 1. Sketch of specific HER2 biodetection based on an SPR-TFBG biofunctionalized using anti-HER2 aptamers.

Prior to the immobilization on the gold-coated surface of the sensor, aptamers were resuspended in TE buffer (Tris-ethylenediaminetetraacetic) 100 µM (Base Pair Biotechnologies) and diluted 1:1 v/v with TCEP (Tris (2-carboxyethyl) phosphine) solution. To achieve the folding into their tertiary structure and then allow an optimal binding to the HER2 protein, a reduction step was carried out at 90 °C for 5 min. The aptamer solution was diluted in Phosphate Buffer Saline (PBS) from Thermo Scientific (pH 7.2) to reach the working concentration of 10.24 µM for the immobilization.

Finally, in order to avoid any unreliable readouts due to non-specific recognitions, the aptasensor surface was blocked with 6-mercapto-1-hexanol (Sigma Aldrich) 5 mM for 30 min in PBS at room temperature (RT). The experimental setup was composed of a LUNA optical vector analyzer (OVA) and a small disposable manufactured container (~30 × 5x4 mm) able to contain

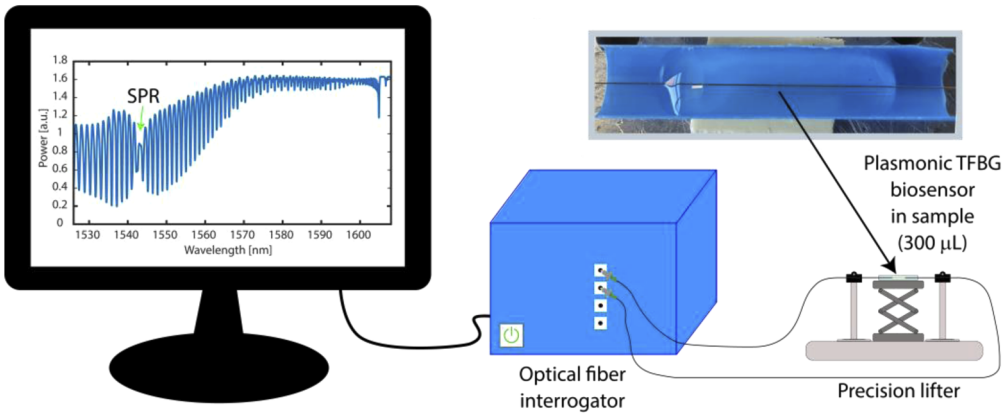

Fig. 2. Scheme of the experimental setup used for biofunctionalization and biodetection experiments (300 µL samples are used).

Biomedical Optics EXPRESS

300 µL sample with the aim to achieve measurements in the transmission configuration (Fig. 2). The biosensor is gently immersed in a given solution by means of a micrometric screw lifter. Samples stay in place in the setup during measurements. Solutions are exchanged by pipetting and translating the sensor.

First experiments concerned the detection by direct interaction between anti-HER2 aptamers grafted onto the sensor surface and the HER2 protein (full recombinant human protein Erb-B2, 116 kDA, from Abcam ab60866) in PBS at RT. The specific interaction between the synthetized aptamers and the HER2 commercial protein was validated by means of lateral flow assays [43]. Then, the HER2 detection was confirmed and amplified using 20 µL/mL polyclonal anti-HER2 antibodies (BOSSBS-2896R from Bioss Antibodies) in PBS.

3. Bioassays results with anti-HER2 antibody signal amplification

3.1. Aptamer immobilization and blocking step tracking

The optical fiber-based sensor gives the possibility to follow the biofunctionalization process prior to the biodetection itself. The sensorgram of the aptamer immobilization was therefore recorded. For the demodulation technique, we use the envelope of the transmission spectra in the wavelength range impacted by the SPR, more precisely the lower envelope passing through the minima of the cladding mode resonances. To this aim we used the envelope function of MATLAB and optimized its parameters to find the envelope curve which match in the best way with our experimental signals. This envelope features the SPR signature that appears as a local maximum. The fitting and tracking of the wavelength shift of this maximum is used in this work to demodulate the biosensor response [Fig. 3(a)]. This method allows to access to very high shifts in comparison with conventional demodulation technique based on individual mode tracking (few dozens of pm) [44,45].

In addition, the use of an SPF is particularly well-suited for the implementation of this technique since light is inline polarized with high extinction ratio. Therefore, the spectrum is not disturbed by residual S-polarized modes and much more robust in practice. SPR excitation usually appears very clean in the spectrum, with a clear attenuation of cladding mode resonances that couple with the plasmon wave. It is therefore rather easy to track the envelope evolution of all the modes as a footprint of the SPR during experiments instead of following individual cladding mode as previously done in classical telecommunication-grade SMF [13].

Measurements were performed in PBS before and after this step showing a wavelength shift of ~100 pm [Figs. 3(b) and 3(d)]. In contrast, a gradual and relatively high wavelength shift up to 300 pm is observed in the aptamer solution which reflects the binding of the aptamers onto the gold surface [Figs. 3(c) and 3(d)]. A covalent binding is expected due to the thiols functional groups present on the synthesized aptamers. The sudden jumps observed from PBS to the aptamer solution result from a difference in term of refractive index values.

The sensorgram of the blocking step was recorded as a function of time [Fig. 4(a) and Fig. 4(b)]. A continuous wavelength shift reaching ~250 pm can be observed during 25 min. Indeed, the small mercaptohexanol molecules progressively form a layer that blocks free spaces between the bioreceptors, and such a layer grows as a function of time. The reaction is stopped after ~25 min which corresponds to the time usually observed for an efficient surface blocking step [19,20,27].

3.2. HER2 aptasensing with antibody amplification

After the sensor surface was chemically blocked against non-specific recognition, detection of the breast cancer biomarker was first performed before achieving an amplification assay through specific polyclonal antibodies (Figs. 5 and 6). For HER2 aptasensing, the sensor was immersed in a 10^{-6} g/mL HER2 solution (in PBS) to examine the interaction with the anti-HER2 aptamers.

Biomedical Optics EXPRESS

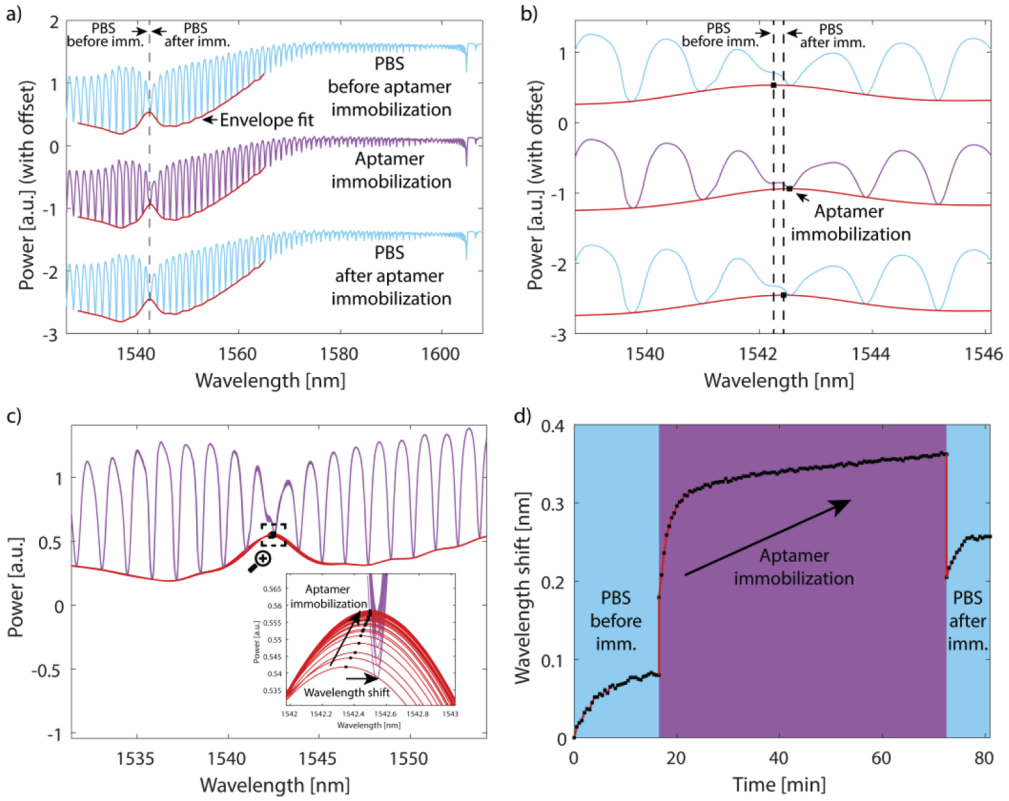

Fig. 3. Response signal of the SPR-TFBG at the end of the aptamer immobilization and in PBS (before and after aptamer grafting) (a) with an enlargement on the spectral region of interest (b). The fit of the SPR signature using the envelope is also shown. Enlargement on the wavelength shift of the SPR envelope maximum around during the aptamer immobilization (c). Sensorgram showing the tracking of the wavelength shift in nm over time of the SPR envelope during the aptamer immobilization with immersion in PBS before and after grafting (d).

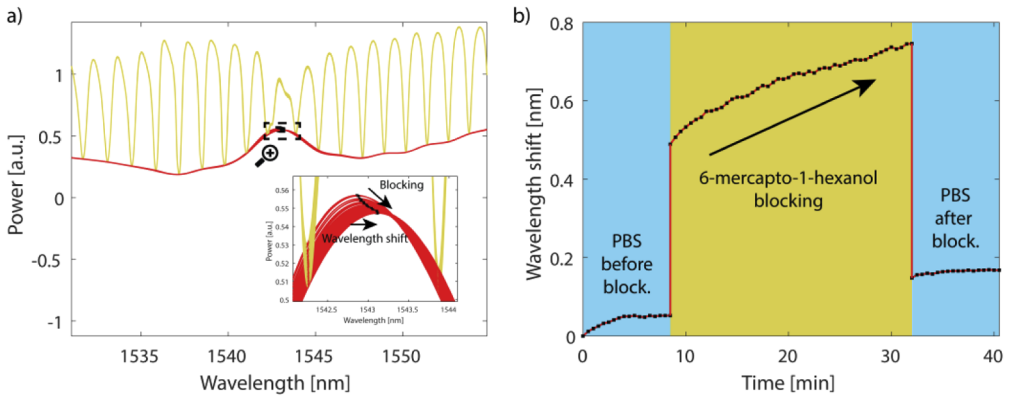

Fig. 4. Tracking of the SPR-TFBG response signal shift in wavelength during the 6-mercapto-1-hexanol blocking in PBS with an enlargement on the spectral region of interest (a). The sensorgram obtained by using the tracking of the maximum of the SPR envelope overtime is also plotted (b).

Biomedical Optics EXPRESS

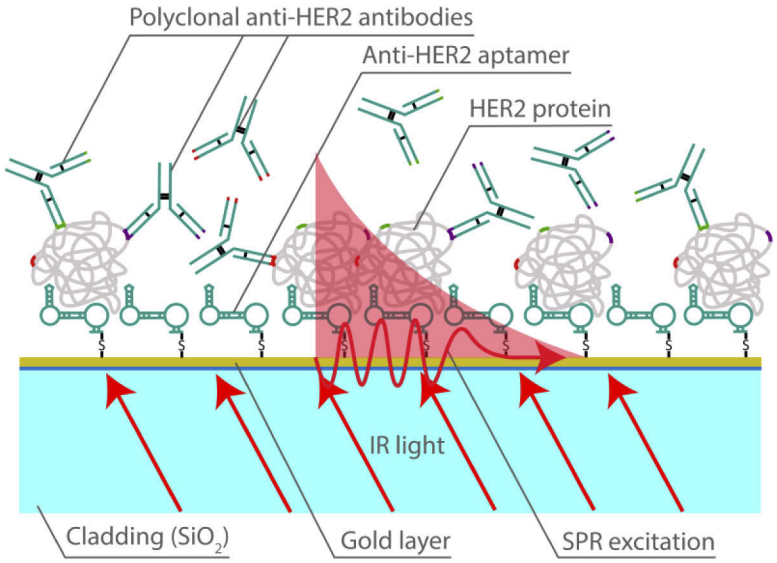

Fig. 5. Sketch of principle of HER2 biodetection at SPR TFBG aptasensor interface through anti-HER2 aptamers and signal amplification using anti-HER2 antibodies.

The tracking of the envelope reveals a progressive wavelength shift of ~300 pm from the beginning of the contact with protein solution until reaching a more stable biochemical equilibrium [Figs. 6(a) and 6(c)]. Indeed, it can be seen in Fig. 6(c) that the incubation time is approximatively 20 min for our aptasensor with the HER2 protein.

The evolution corresponding to the first part of the curve can be explained by a rapid and specific interaction between proteins and aptamers. Then, a close proximity to the biochemical balance is progressively reached in the second part, since the aptamer layer is progressively saturated by HER2.

In order to amplify and confirm the HER2 aptadetection, a signal amplification was achieved by bringing the tested sensor into contact with a solution of anti-HER2 antibodies. The advantage of using antibodies (~ 150 kDa) in this sandwich assay is to benefit from a higher molecular weight in comparison with aptamers (~ 12 kDa) which increase the amplification response. In addition, the use of polyclonal antibodies allows several bindings with a given protein which also impacts positively the amplification assay.

A rinsing step in PBS was done to remove unbound proteins coming from the first detection and polyclonal antibodies were therefore chosen to allow more specific antibodies-HER2 interactions. The sensorgram of this assay shows a high wavelength shift of ~800 pm, which represents more than two and a half times the shift observed in the case of the aptamers-HER2 interactions [Figs. 6(b) and 6(c)].

Biomedical Optics EXPRESS

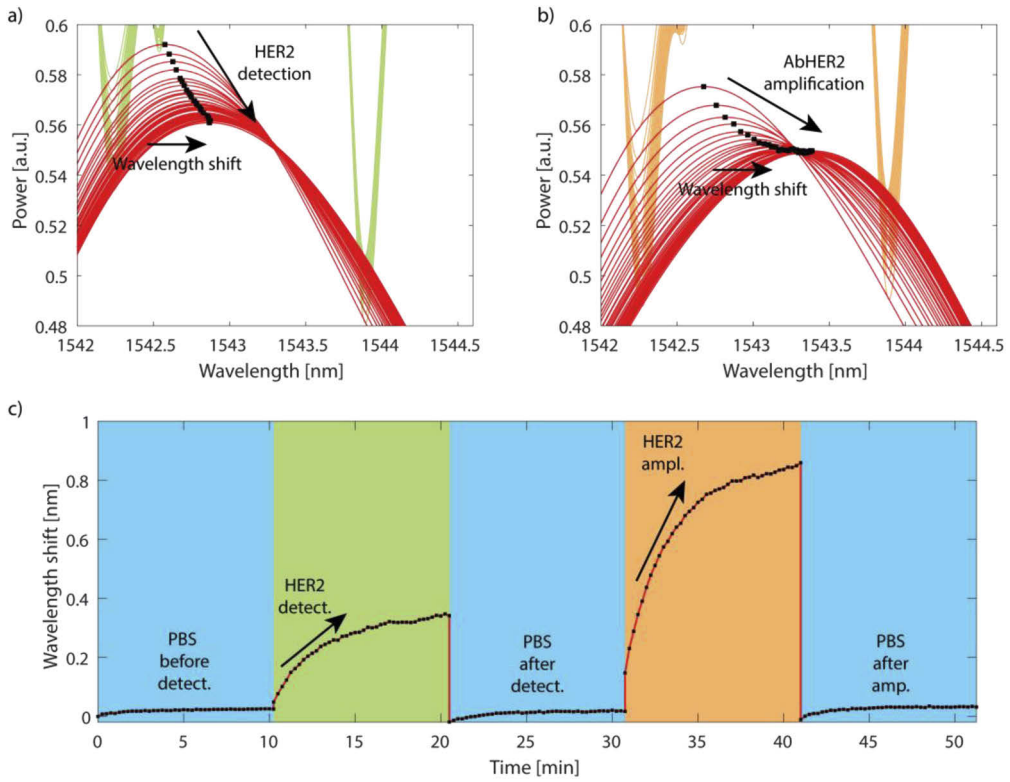

Fig. 6. Tracking of the SPR envelope in the spectral region of interest during the HER2 biodetection through anti-HER2 aptamers (a) and the anti-HER2 amplification (b). Tracking of the wavelength shift in nm over time of the maximum of the SPR envelope during the biodetection with measurements in PBS between each step (c).

4. Conclusion

Titled fiber Bragg gratings coupled to the plasmonic effect are of growing interest in the biomedical detection field due to their indisputable advantages allowing to foresee real time measurement in point-of-care with miniaturized probes. Our work investigated a new approach to analyze the plasmonic response of TFBG sensors turned into biosensors. We oriented our sensor against the HER2 protein, a relevant biomarker whose presence is assessed in routine for the diagnosis of the most aggressive forms of breast cancer. Our demodulation technique based on tracking the local maximum of the lower envelope of the SPR-TFBG spectrum leads to wavelength shifts that are much higher than conventional method. A ~300 pm red-shift is observed during the HER2 aptamer-protein interaction where this value does not exceed few tens of pm in case of traditional mode tracking methods. This is because we track a spectral feature as close as possible to the actual SPR. An amplification of the detection was achieved by using anti-HER2 antibodies and led to a high extra shift of ~800 pm. Optical fiber-based sensors also enable the following of the bioreceptor immobilization in real-time during the biofunctionalization. Experiments were significantly fostered using SPF which directly allows inline P-polarization state required for SPR excitation. Experimental readouts also gain in robustness and quality thanks to the intrinsic structure of this specialty fiber which makes the core guided light less sensitive to optical fiber bending. The response observed in this work highlights therefore the potential of an envelope-based demodulation technique for the data analysis, showing relevant and interesting features for further on-site and convenient biosensing.

Biomedical Optics EXPRESS

Funding

Fonds De La Recherche Scientifique - FNRS (O001518F).

Acknowledgment

The authors are grateful to Mariel David for her help in preparing optical fiber-based sensors. This work was financially supported by the Fonds de la Recherche Scientifique – FNRS under Grant n° O001518F (EOS-convention 30467715), FRIA Grant of M. Loyez (FRS-FNRS) and Grant of the Associate Researcher position of C. Caucheteur (FRS-FNRS).

Disclosures

The authors declare that there are no conflicts of interest related to this article.

References

1. B. Lee, "Review of the present status of optical fiber sensors," Opt. Fiber Technol. **9**(2), 57–79 (2003).
2. J. P. Dakin, K. Hotate, R. A. Lieberman, and M. A. Marcus, "Optical fiber sensor," in *Handbook of Optoelectronics*, J. P. Dakin and R. G. W. Brown, eds., 2nd ed. (CRC Press, 2017), pp. 1–84.
3. K. T. V. Grattan and Y. N. Ning, "Optical current sensor technology," in *Optical Fiber Sensor Technology*, K. T. V. Grattan and B. T. Meggitt, eds., 1st ed. (Springer, 1998), pp. 183–223.
4. T. Guo, F. Liu, B. O. Guan, and J. Albert, "Tilted fiber grating mechanical and biochemical sensors," Opt. Laser Technol. **78**, 19–33 (2016).
5. Z. Li, Z. Yu, Y. Shen, X. Ruan, and Y. Dai, "Graphene enhanced leaky mode resonance in tilted fiber Bragg grating: a new opportunity for highly sensitive fiber optic sensor," IEEE Access **7**, 26641–26651 (2019).
6. Z. Li, J. Shen, Q. Ji, X. Ruan, Y. Zhang, Y. Dai, and Z. Cai, "Tuning the resonance of polarization-degenerate LP1,l cladding mode in excessively tilted long period fiber grating for highly sensitive refractive index sensing," J. Opt. Soc. Am. A **35**(3), 397–405 (2018).
7. F. Ouellette, J. Li, Z. Ou, and J. Albert, "High-resolution interrogation of tilted fiber Bragg gratings using an extended range dual wavelength differential detection," Opt. Express **28**(10), 14662 (2020).
8. S. Poeggel, D. Tosi, D. Duraibabu, G. Leen, D. McGrath, and E. Lewis, "Optical fibre pressure sensors in medical applications," Sensors **15**(7), 17115–17148 (2015).
9. O. V. Butov, A. P. Bazakutsa, Y. K. Chamorovskiy, A. N. Fedorov, and I. A. Shevtsov, "All-fiber highly sensitive Bragg grating bend sensor," Sensors **19**(19), 4228 (2019).
10. C. Christopher, A. Subrahmanyam, and V. V. R. Sai, "Gold sputtered U-bent plastic optical fiber probes as SPR- and LSPR-based compact plasmonic sensors," Plasmonics **13**(2), 493–502 (2018).
11. A. Iadicicco, A. Cutolo, S. Campopiano, M. Giordano, and A. Cusano, "Advanced fiber optical refractometers based on partially etched fiber Bragg gratings," 1218–1221 (2004).
12. C. Caucheteur, T. Guo, and J. Albert, "Review of plasmonic fiber optic biochemical sensors: improving the limit of detection," Anal. Bioanal. Chem. **407**(14), 3883–3897 (2015).
13. M. Lobry, D. Lahem, M. Loyez, M. Debliquy, K. Chah, M. David, and C. Caucheteur, "Non-enzymatic D-glucose plasmonic optical fiber grating biosensor," Biosens. Bioelectron. **142**, 111506 (2019).
14. F. Chiavaioli, F. Baldini, S. Tombelli, C. Trono, and A. Giannetti, "Biosensing with optical fiber gratings," Nanophotonics **6**(4), 663–679 (2017).
15. T. Guo, "Fiber grating-assisted surface plasmon resonance for biochemical and electrochemical sensing," J. Lightwave Technol. **35**(16), 3323–3333 (2017).
16. M. E. Bosch, A. J. R. Sánchez, F. S. Rojas, and C. B. Ojeda, "Recent development in optical fiber biosensors," Sensors **7**(6), 797–859 (2007).
17. J. H. Qu, A. Dillen, W. Saeys, J. Lammertyn, and D. Spasic, "Advancements in SPR biosensing technology: An overview of recent trends in smart layers design, multiplexing concepts, continuous monitoring and in vivo sensing," Anal. Chim. Acta **1104**, 10–27 (2020).
18. M. jie Yin, B. Gu, Q. F. An, C. Yang, Y. L. Guan, and K. T. Yong, "Recent development of fiber-optic chemical sensors and biosensors: Mechanisms, materials, micro/nano-fabrications and applications," Coord. Chem. Rev. **376**, 348–392 (2018).
19. M. Loyez, E. M. Hassan, M. Lobry, F. Liu, and C. Caucheteur, "Rapid detection of circulating breast cancer cells using a multi-resonant optical fiber aptasensor with plasmonic amplification," ACS Sens. **5**(2), 454–463 (2020).
20. M. Loyez, M. Lobry, R. Wattiez, and C. Caucheteur, "Optical fiber gratings immunoassays," Sensors **19**(11), 2595 (2019).
21. R. L. Siegel, K. D. Miller, and A. Jemal, "Cancer statistics," CA. Cancer J. Clin. **68**(1), 7–30 (2018).
22. T. Doi, K. Shitara, Y. Naito, A. Shimomura, Y. Fujiwara, K. Yonemori, C. Shimizu, T. Shimoi, Y. Kuboki, N. Matsubara, A. Kitano, T. Jikoh, C. Lee, Y. Fujisaki, Y. Ogitani, A. Yver, and K. Tamura, "Safety, pharmacokinetics,

Biomedical Optics EXPRESS

and antitumour activity of trastuzumab deruxtecan (DS-8201), a HER2-targeting antibody–drug conjugate, in patients with advanced breast and gastric or gastro-oesophageal tumours: a phase 1 dose-escalation study," Lancet Oncol. **18**(11), 1512–1522 (2017).
23. K. Araki and Y. Miyoshi, "Mechanism of resistance to endocrine therapy in breast cancer: the important role of PI3 K/Akt/mTOR in estrogen receptor-positive, HER2-negative breast cancer," Breast Cancer **25**(4), 392–401 (2018).
24. V. Belli, N. Matrone, S. Napolitano, G. Migliardi, F. Cottino, A. Bertotti, L. Trusolino, E. Martinelli, F. Morgillo, D. Ciardiello, V. De Falco, E. F. Giunta, U. Bracale, F. Ciardiello, and T. Troiani, "Combined blockade of MEK and PI3KCA as an effective antitumor strategy in HER2 gene amplified human colorectal cancer models," J. Exp. Clin. Cancer Res. **38**(1), 236 (2019).
25. J. S. Ross, J. A. Fletcher, G. P. Linette, J. Stec, E. Clark, M. Ayers, W. F. Symmans, L. Pusztai, and K. J. Bloom, "The HER-2/ neu gene and protein in breast cancer 2003: biomarker and target of therapy," Oncologist **8**(4), 307–325 (2003).
26. D. L. Nielsen, M. Andersson, and C. Kamby, "HER2-targeted therapy in breast cancer. Monoclonal antibodies and tyrosine kinase inhibitors," Cancer Treat. Rev. **35**(2), 121–136 (2009).
27. C. Ribaut, M. Loyez, J. C. Larrieu, S. Chevineau, P. Lambert, M. Remmelink, R. Wattiez, and C. Caucheteur, "Cancer biomarker sensing using packaged plasmonic optical fiber gratings: towards in vivo diagnosis," Biosens. Bioelectron. **92**, 449–456 (2017).
28. T. Erdogan and J. E. Sipe, "Tilted fiber phase gratings," J. Opt. Soc. Am. A **13**(2), 296 (1996).
29. C. Chan, C. Chen, A. Jafari, A. Laronche, D. J. Thomson, and J. Albert, "Optical fiber refractometer using narrowband cladding-mode resonance shifts," Appl. Opt. **46**(7), 1142–1149 (2007).
30. J. Albert, L. Shao, and C. Caucheteur, "Tilted fiber Bragg grating sensors," Laser Photonics Rev. **7**(1), 83–108 (2013).
31. A. Iadicicco, S. Campopiano, A. Cutolo, M. Giordano, and A. Cusano, "Refractive index sensor based on microstructured fiber Bragg grating," IEEE Photonics Technol. Lett. **17**(6), 1250–1252 (2005).
32. F. Chiavaioli, C. A. J. Gouveia, P. A. S. Jorge, and F. Baldini, "Towards a uniform metrological assessment of grating-based optical fiber sensors: from refractometers to biosensors," Biosensors **7**(4), 23–29 (2017).
33. V. Bhatia and A. M. Vengsarkar, "Optical fiber long-period grating sensors," Opt. Lett. **21**(9), 692–694 (1996).
34. G. Laffont and P. Ferdinand, "Tilted short-period fibre-Bragg-grating-induced coupling to cladding modes for accurate refractometry," Meas. Sci. Technol. **12**(7), 765–770 (2001).
35. K. A. Tomyshev, E. S. Manuilovich, D. K. Tazhetdinova, E. I. Dolzhenko, and O. V. Butov, "High-precision data analysis for TFBG-assisted refractometer," Sens. Actuators, A **308**, 112016 (2020).
36. B. Spackova and J. Homola, "Theoretical analysis of a fiber optic surface plasmon resonance sensor utilizing a Bragg grating," Opt. Express **17**(25), 23254–23264 (2009).
37. C. Caucheteur, V. Voisin, and J. Albert, "Near-infrared grating-assisted SPR optical fiber sensors: design rules for ultimate refractometric sensitivity," Opt. Express **23**(3), 2918–2932 (2015).
38. Y. Schevchenko, T. J. Francis, D. A. D. Blair, R. Walsh, M. C. DeRosa, and J. Albert, "In situ biosensing with a surface plasmon resonance fiber grating aptasensor," Anal. Chem. **83**(18), 7027–7034 (2011).
39. X. Chen, Y. Nan, X. Ma, H. Liu, W. Liu, L. Shi, and T. Guo, "In-Situ detection of small biomolecule interactions using a plasmonic tilted fiber grating sensor," J. Lightwave Technol. **37**(11), 2792–2799 (2019).
40. V. Márquez-Cruz and J. Albert, "High resolution NIR TFBG-assisted biochemical sensors," J. Lightwave Technol. **33**(16), 3363–3373 (2015).
41. E. M. Hassan, W. G. Willmore, B. C. Mckay, and M. C. DeRosa, "In vitro selections of mammaglobin A and mammaglobin B aptamers for the recognition of circulating breast tumor cells," Sci. Rep. **7**(1), 14487 (2017).
42. M. Gijs, G. Penner, G. B. Blackler, N. R. E. N. Impens, S. Baatout, A. Luxen, and A. M. Aerts, "Improved aptamers for the diagnosis and potential treatment of HER2-positive cancer," Pharmaceuticals **9**(2), 29 (2016).
43. V. Ranganathan, S. Srinivasan, A. Singh, and M. C. DeRosa, "An aptamer-based colorimetric lateral flow assay for the detection of human epidermal growth factor receptor 2 (HER2)," Anal. Biochem. **588**, 113471 (2020).
44. E. Manuylovich, K. Tomyshev, and O. V. Butov, "Method for determining the plasmon resonance wavelength in fiber sensors based on tilted fiber Bragg gratings," Sensors **19**(19), 4245 (2019).
45. M. Loyez, C. Ribaut, C. Caucheteur, and R. Wattiez, "Chemical Functionalized gold electroless-plated optical fiber gratings for reliable surface biosensing," Sens. Actuators, B **280**, 54–61 (2019).